Article

Modification of tomato breeding traits and plant hormone signaling by Target-AID, the genome-editing system inducing efficient nucleotide substitution

Sachiko Kashojiya[1,2,†], Yu Lu[1,2,†], Mariko Takayama[1], Hiroki Komatsu[1], Luyen Hieu Thi Minh[1], Keiji Nishida[3,4], Kenta Shirasawa[5], Kenji Miura[1], Satoko Nonaka[1], Jun-ichiro Masuda[1,6], Akihiko Kondo[3,4], Hiroshi Ezura[1,7,*] and Tohru Ariizumi[1,7,*]

[1]Faculty of Life and Environmental Sciences, University of Tsukuba, Gene Research Center, Tsukuba, Ibaraki 305-8572, Japan
[2]Japan Society for Promotion of Science, 5-3-1, Kojimachi, Tokyo 102-0083, Japan
[3]Graduate School of Science, Technology and Innovation, Kobe University, 1-1 Rokkodai, Nada, Kobe, Hyogo 657-8501, Japan
[4]Engineering Biology Research Center, Kobe University, 7-1-49, Minatojima Minami Machi, Chuo-ku, Kobe 650-0047, Japan
[5]Kazusa DNA Research Institute, 2-6-7 Kazusa-Kamatari, Kisarazu, Chiba 292-0818, Japan
[6]Faculty of Agriculture, University of Miyazaki, 1-1 Gakuenkibanadai-nishi, Miyazaki, Miyazaki 889-2192, Japan
[7]Tsukuba Plant Innovation Research Center, University of Tsukuba, Ibaraki 305-8572, Japan

*Corresponding authors. E-mail: ezura.hiroshi.fa@u.tsukuba.ac.jp; ariizumi.toru.ge@u.tsukuba.ac.jp.
[†]These authors have contributed equally to this work.

Abstract

Target activation-induced cytidine deaminase (Target-AID), a novel CRISPR/Cas9-based genome-editing tool, confers the base-editing capability on the Cas9 genome-editing system. It involves the fusion of cytidine deaminase (CDA), which catalyzes cytidine (C) to uridine (U) substitutions, to the mutated nickase-type nCas9 or deactivated-type dCas9. To confirm and extend the applicability of the Target-AID genome-editing system in tomatoes (*Solanum lycopersicum* L.), we transformed the model tomato cultivar "Micro-Tom" and commercial tomato cultivars using this system by targeting *SlDELLA*, which encodes a negative regulator of the plant phytohormone gibberellic acid (GA) signaling pathway. We confirmed that the nucleotide substitutions were induced by the Target-AID system, and we isolated mutants showing high GA sensitivity in both "Micro-Tom" and the commercial cultivars. Moreover, by successfully applying this system to *ETHYLENE RECEPTOR 1* (*SlETR1*) with single sgRNA targeting, double sgRNA targeting, as well as dual-targeting of both *SlETR1* and *SlETR2* with a single sgRNA, we demonstrated that the Target-AID genome-editing system is a promising tool for molecular breeding in tomato crops. This study highlights an important aspect of the scientific and agricultural potential of the combinatorial use of the Target-AID and other base-editing systems.

Introduction

In prokaryotes, clustered regularly interspaced short palindromic repeat (CRISPR)-associated endonuclease 9 (CRISPR/Cas9) system functions as an adaptive immune system that modifies the genome [1]. The CRISPR/Cas9 derived genome-editing system is composed of the Cas9 endonuclease and a single guide RNA (sgRNA) that targets specific loci of interest on the genome. Owing to the simplicity of sgRNA designation, the CRISPR/Cas9 system is the most popular genome-editing tool and is widely applied to both animals and plants [2, 3]. It induces double-strand breaks (DSBs) at specific sites; subsequently, the activity of the error-prone non-homologous end-joining (NHEJ) DNA repair system results in the introduction of insertions and deletions (indels) at the target site, leading to a knockout or knockdown of the target gene. In contrast, a base editor that introduces a precise nucleotide substitution has

been developed by fusing the base-editing enzyme to a mutated Cas9 (mCas9) protein that lacks endonuclease activity, partially (nickase Cas9 or nCas9) or completely (dead Cas9 or dCas9) [4, 5]. The cytidine deaminase (CDA) protein and engineered adenine base editor (ABE) protein provide C-to-T and A-to-G nucleotide substitution ability to the CRISPR-Cas9 system, respectively [6–9]. Furthermore, it has been demonstrated that fusion of uracil DNA glycosylase inhibitor (UGI) [10] to CDA can improve the base-editing efficiency because it blocks uracil DNA glycosylase-catalyzed removal of uracil (U), preventing U:G mismatch from being repaired to the original C:G pair. Besides, the 2A peptide-encoding sequence (coding for a foot-and-mouth disease virus 2A peptide) [11] is often used to coexpress genes upstream and downstream draftrulesof it to ensure simultaneous gene expression for two different genes using a single transformation vector. Thus, when Cas9 and antibiotic marker genes are

joined with the 2A peptide-encoding sequence, we can expect the transgenic plants with antibiotic resistance to express Cas9. Although it is desirable to evaluate the feasibility of use and applicability of these components (UGI and 2A peptide), their comprehensive evaluation in plants has been limited.

The Target-AID system, which acts as a base editor that induces a C-to-T nucleotide substitution, was developed and verified in yeast and mammalian cells [7]. Recently, we reported that this genome-editing system induces a point mutation in the tomato (*Solanum lycopersicum*) cultivar "Micro-Tom", by targeting the *SlDELLA* and *SlETR1* genes [12]. However, a detailed characterization of the genome-edited tomato plants has not yet been reported. Moreover, although genome-editing technology has been adapted to model lines in various crops, adaptation to commercial varieties is an important issue that needs to be checked. Thus, the feasibility of using this system in commercial tomato cultivars should be evaluated.

Parthenocarpy, the formation of fruits without prior pollination and fertilization, is an essential agricultural trait that profoundly affects production efficiency and cost [13]. The mechanism regulating fruit set involves the crosstalk of multiple plant hormones, including gibberellic acid (GA), which promotes the division of cells and the growth of ovaries after pollination [14, 15, 16]. GA also regulates many aspects of growth in tomato, including internode growth, leaf shape, and style length [14–15]. The over-accumulation of GA or the activation of GA signaling by genetic mutation, as well as direct application of GA to the ovaries, induces parthenocarpy in tomato plants [14, 15, 17].

The DELLA protein negatively regulates GA signaling by inhibiting its downstream component. The inhibitory regulation of GA signaling is released by the formation of the GA–GID1–DELLA complex, which is subsequently recognized by the ubiquitination system, leading to the ubiquitination and proteasomal degradation of DELLA [18, 19]. DELLA belongs to a subgroup of GRAS proteins containing the highly conserved C-terminal GRAS domain. In tomatoes, GA signaling is solely regulated by a single *SlDELLA* gene, also called *PROCERA*, and the loss-of-function mutant that lacks the conserved GRAS domain accounts for 95% of the GA-signaling response, including parthenocarpy [20]. A natural tomato mutant, *procera*, translates the SlDELLA^{V302E} protein, harboring a point mutation in the conserved VHIID subdomain of the GRAS domain, and shows strongly activated GA signaling and the formation of parthenocarpic fruit [17]. Recently, using EMS mutagenesis, we isolated a mutant harboring a novel point mutation in *SlDELLA* named *procera-2*, which translates SlDELLA^{L567F} with a point mutation in the SAW subdomain of the GRAS domain.

The *procera-2* mutant shows efficient parthenocarpy; it exhibits relatively milder GA-related phenotypes and apparently carries fewer unfavorable breeding traits compared with that in the *procera* mutant in the

genetic background of "Micro-Tom" [21]. For example, unfavorable phenotype, such as lesser number of flowers in *procera* compared with that in wild-type (WT) plants, is largely alleviated in the *procera-2* mutant. Furthermore, fruit productivity in the *procera-2* mutant after 2 months of heat stress is higher than that in the *procera* mutant, which is likely due to the higher number of flowers formed compared with that in the *procera* mutant [17]. These results suggest that the SAW subdomain of the *SlDELLA* gene would be a desirable target site for genome editing to improve breeding traits and confer parthenocarpy without the associated unfavorable breeding traits. Therefore, to validate the applicability of the Target-AID base-editing system, we targeted the *procera-2* mutation site, aiming to get a variation of the point mutations expected to generate tomatoes with a variety of GA sensitivity and parthenocarpy in both "Micro-Tom" and commercial tomato cultivars.

In this study, we developed a series of *SlDELLA*-edited tomato plants using the Target-AID system and examined, in detail, the characteristics of the genome-editing spectra as well as GA-related phenotypes, including parthenocarpy, in different genetic backgrounds, including F$_1$ hybrids, in selected commercial cultivars. Moreover, in addition to *SlDELLA*, we report the application of this strategy for targeting the ethylene receptor *SlETR1* gene, as well as for multi-target genome editing. Finally, we present an assessment of the potential use of a combination of advanced genome-editing tools for agricultural application.

Results and discussion
Characteristics of mutation spectra induced by target-AID in "micro-tom" tomatoes

To design the Target-AID vectors, the mutated *Cas9*, *nCas9* (D10A), and *dCas9* (D10A H840A) [4,5] were fused with sea lamprey *CDA1* [8,9]; both human codon-optimized *CDA1*^{Hs} and *Arabidopsis thaliana* codon-optimized *CDA1*^{At} variations were used (Fig. 1a). *dCas9-CDA1*^{At} was fused with a uracil glycosylase inhibitor (*UGI*) [10] to create *dCas9-CDA1*^{At}*-UGI*, with an aim to improve the frequency of base-editing. In addition to the Target-AID vectors, the conventional CRISPR-Cas9 vector, *Cas9*, was used as a control in this study. The *nCas9* has a stop codon before the translational start codon of CDA, thereby facilitating its use as a negative control for the experiment. We designed sgRNAs to target four endogenous tomato genes [18, 22–24]: *SlDELLA* (*Solyc11g011260*), *SlETR1* (*Solyc12g011330*), *SlETR2* (*Solyc07g056580*), and *Hawaiian skirt* (*SlHWS*, *Solyc01g095370*). Among these sgRNAs, *SlDELLA*^{T1} targeted *SlDELLA*; *SlETR1*^{T1}, *SlETR1*^{T3}, and *SlETR1*^{T4} targeted *SlETR1*; *SlETR1*^{T2} targeted both *SlETR1* and its homolog *SlETR2* (because they share the same target sgRNA sequence); and *SlHWS*^{T1} and *SlHWS*^{T2} targeted *SlHWS* (Fig. 1b). The combination of these sgRNAs and the genome-editing tools (*Cas9*, *nCas9*, and Target-AID vectors) are shown in Fig. S1.
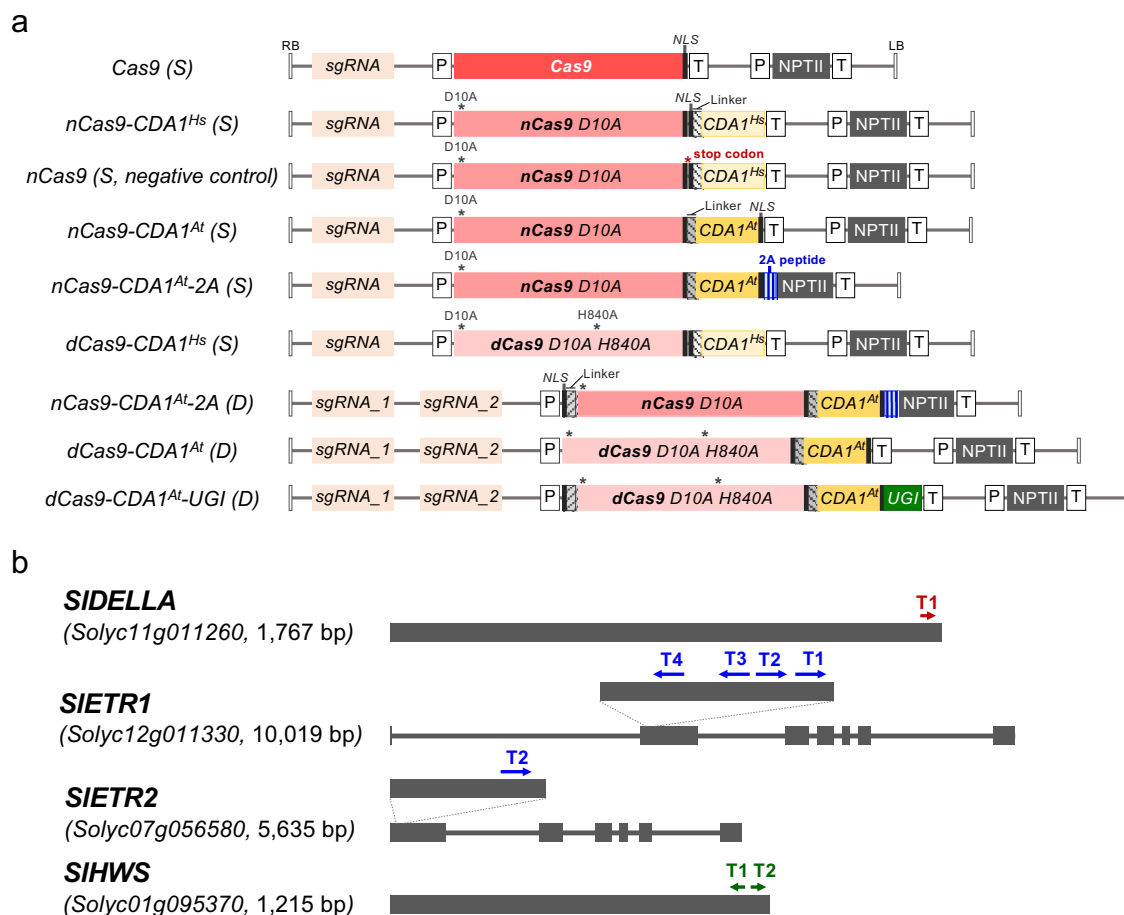
a

b

Figure 1. Target sites in *SlDELLA*, *SlETR1*, *SlETR2*, and *SlHWS* and vector structures for genome editing. **a** Vector name followed by S or *D* in the parentheses, indicates single (S) sgRNA or double (D) sgRNAs. The sgRNAs were expressed under the *AtU6* promoter. The *Cas9* or modified *Cas9s* were expressed under *Petroselinum crispum* (*Pc*) *Ubi* promoter and *Pea3A* terminator, and *NPTII* was expressed under *CMV35S* promoter and *Oryza sativa* (*Os*) *HSP17* terminator. Mutation sites, D10A and H840A, are indicated with asterisks. *Cas9*, CRISPR associated protein 9; *dCas9*, dead Cas9; *nCas9*, nickase Cas9; *CDA1*, cytidine deaminase 1; *UGI*, uracil glycosylase inhibitor; *NPTII*, neomycin phosphotransferase II; *P*, promoter; *T*, terminator; RB, right border; LB, left border; *NLS*, nuclear localization signal; [Hs], Human codon optimized; [At], Arabidopsis codon optimized. **b** The genome structure and target sites of *SlDELLA* (*Sloyc11g011260*), *SlETR1* (*Solyc12g011330*), *SlETR2* (*Solyc07g056580*), and *SlHWS* (*Solyc01g095370*). Box, exon; line, intron; T, target; arrow, target site.

To investigate the characteristics of genome-editing efficiency induced by Target-AID, we targeted the SAW subdomain of SlDELLA (*SlDELLA*[T1]) in the model tomato cultivar "Micro-Tom" using five vectors: *Cas9*, *nCas9-CDA1*[Hs], *nCas9-CDA1*[At], *dCas9-CDA1*[Hs], and *nCas9* (Fig. 1 and Fig. S1). The *SlDELLA* target site was selected based on a previous report on an EMS mutant, *procera-2*, that carries a novel point mutation, L567F, in the SAW subdomain; it also shows a relatively mild parthenocarpy and unfavorable phenotypes compared with the strong phenotype of the *procera* mutant [21]. By targeting the *procera-2* mutation site, we aimed to generate a variety of point mutations that lead to distinct parthenocarpy and GA-related phenotypes due to the different types of amino acid substitutions. All five vectors showed positive *Agrobacterium*-mediated transformation and T0 plants that possessed T-DNA insertion could be obtained from all the vectors (Tables S1 and S2). We have previously conducted a similar scheme of study in which these vectors were used. In this study, we used 20 transformants from previous studies [12] and 30 newly created transformants for further analysis (Tables S1, S3, and S4).

The results of Sanger sequencing showed that three vectors, *Cas9*, *nCas9-CDA1*[Hs], and *nCas9-CDA1*[At], induced genome editing at the target site in T0 and T1 plants more efficiently than the *nCas9* negative control vector. An indel editing pattern occurred in *Cas9*, and both indel and nucleotide substitution occurred in *nCas9-CDA1*[Hs] and *nCas9-CDA1*[At] (Tables S1–S4). In contrast, the *dCas9-CDA1*[Hs] vector induced genome editing in only one of the nine T0 plants analyzed, and none of the T1 progenies from this line showed genome-edited mutations (Table S1).

Next, to characterize the genome editing pattern of the SlDELLA protein induced by the Target-AID system in detail, the genome-edited T0 plants from the *nCas9-CDA1*[Hs] and *nCas9-CDA1*[At] vectors were selected, and the sequences of ON-target and OFF-target sites were analyzed using the Illumina Mi-Seq system. The analysis

Table 1. Target-sequencing analysis of T_0 $SlDELLA^{T1}$ edited plants that were edited using *Cas9*, Target-AID, and *nCas9* vectors in ON-target and OFF-target sites

$SlDELLA^{T1}$ ON-Target (PAM positions at right)

Name	Rate of indel (%)		C	A	C	T	T	A	T	A	G	C	T	A	C	C	T	C	C	G	C	C	T	G	G
Cas9 #31	46.1	T	0.2	0.0	0.1	99.9	99.9	0.0	100.0	0.0	0.1	0.0	99.9	0.0	0.0	0.2	99.7	0.1	0.1	0.2	0.0	0.0	99.8	0.1	0.5
		G	0.0	0.0	0.3	0.1	0.1	0.0	0.0	0.0	99.8	0.0	0.0	0.0	0.0	0.0	0.0	0.0	0.0	96.1	0.0	0.0	0.1	99.8	99.1
		C	99.7	0.2	99.7	0.0	0.0	0.0	0.0	0.3	0.0	99.7	0.0	0.0	99.9	99.6	0.2	99.3	92.3	0.0	65.7	99.9	0.0	0.0	0.2
		A	0.0	99.7	0.0	0.0	0.0	100.0	0.0	99.6	0.0	0.2	0.0	99.9	0.1	0.2	0.0	0.1	0.0	0.1	0.0	0.0	0.0	0.1	0.2
nCas9-CDA1^Hs #1	3.5	T	48.2	0.0	3.9	99.8	99.9	0.0	100.0	0.0	0.1	0.1	99.9	0.0	0.2	0.1	99.8	0.1	0.3	0.2	0.0	0.0	99.5	0.0	0.7
		G	0.1	0.0	46.8	0.1	0.1	0.0	0.1	0.0	99.9	0.1	0.0	0.0	0.0	0.1	0.0	0.0	0.0	99.7	0.0	0.0	0.3	99.9	98.8
		C	51.7	0.2	49.2	0.0	0.0	0.0	0.0	0.2	0.0	99.6	0.1	0.0	99.7	99.7	0.1	99.6	99.4	0.0	99.8	99.8	0.1	0.0	0.2
		A	0.0	99.7	0.0	0.1	0.1	99.9	0.0	97.4	0.0	0.2	0.0	99.9	0.1	0.1	0.0	0.1	0.0	0.0	0.0	0.1	0.0	0.0	0.3
nCas9-CDA1^At #3	23.5	T	30.5	0.0	54.4	99.8	99.8	0.0	100.0	0.0	0.1	0.1	99.8	0.1	0.1	0.1	99.8	0.2	0.3	0.2	0.1	0.0	99.7	0.0	0.7
		G	0.2	0.0	5.1	0.1	0.1	0.0	0.0	0.0	99.7	0.1	0.0	0.0	0.0	0.0	0.0	0.1	0.0	99.7	0.0	0.0	0.0	99.8	98.9
		C	69.4	0.4	40.5	0.0	0.0	0.0	0.0	0.1	0.0	99.7	0.1	0.0	99.8	99.8	0.1	99.6	99.6	0.0	99.9	99.9	0.1	0.0	0.1
		A	0.0	99.6	0.0	0.0	0.0	99.9	0.0	76.9	0.0	0.0	0.1	99.9	0.1	0.1	0.0	0.1	0.0	0.0	0.0	0.0	0.0	0.0	0.1
dCas9-CDA1^Hs #3	0.6	T	0.7	0.0	0.2	99.7	99.8	0.0	100.0	0.0	0.0	0.1	99.9	0.0	0.0	0.1	99.9	0.1	0.2	0.2	0.0	0.0	99.7	0.1	0.9
		G	0.1	0.0	0.6	0.1	0.1	0.0	0.0	0.0	100.0	0.0	0.0	0.0	0.0	0.0	0.0	0.0	0.0	99.8	0.0	0.0	0.2	99.8	98.6
		C	99.2	0.2	99.2	0.1	0.1	0.0	0.0	0.3	0.0	99.7	0.0	0.0	99.8	99.8	0.1	99.8	99.6	0.0	99.6	99.9	0.1	0.0	0.2
		A	0.0	99.8	0.0	0.0	0.0	100.0	0.0	99.6	0.0	0.2	0.0	100.0	0.2	0.0	0.0	0.1	0.0	0.0	0.0	0.0	0.0	0.1	0.3
nCas9 #4-2	0.1	T	0.1	0.0	0.2	99.9	99.8	0.0	100.0	0.0	0.1	0.1	99.9	0.0	0.0	0.1	99.9	0.1	0.1	0.2	0.0	0.0	99.7	0.0	0.9
		G	0.0	0.0	0.1	0.1	0.1	0.0	0.0	0.0	99.9	0.0	0.0	0.0	0.0	0.0	0.0	0.0	0.0	99.7	0.0	0.0	0.2	99.9	98.8
		C	99.9	0.2	99.7	0.0	0.1	0.0	0.0	0.3	0.0	99.7	0.1	0.0	99.9	99.8	0.1	99.8	99.8	0.0	99.9	99.9	0.1	0.0	0.2
		A	0.0	99.7	0.0	0.0	0.0	99.9	0.0	99.6	0.0	0.2	0.0	100.0	0.1	0.1	0.0	0.1	0.0	0.1	0.0	0.0	0.0	0.1	0.1
WT	0.3	T	0.1	0.0	0.2	99.9	99.9	0.0	100.0	0.0	0.1	0.0	100.0	0.0	0.0	0.1	99.9	0.1	0.2	0.1	0.0	0.0	99.8	0.0	0.8
		G	0.0	0.0	0.1	0.1	0.1	0.0	0.0	0.0	99.9	0.0	0.0	0.0	0.0	0.0	0.0	0.0	0.0	99.8	0.0	0.0	0.1	99.9	98.9
		C	99.9	0.2	99.6	0.0	0.1	0.0	0.0	0.3	0.0	99.7	0.0	0.0	99.9	99.8	0.1	99.8	99.7	0.0	100.0	99.9	0.1	0.0	0.2
		A	0.0	99.8	0.0	0.0	0.0	100.0	0.0	99.5	0.0	0.2	0.0	100.0	0.1	0.1	0.0	0.1	0.0	0.0	0.0	0.0	0.0	0.0	0.1

$SlDELLA^{T1}$ OFF-Target (PAM positions at right)

Name	Rate of indel (%)		T	A	C	T	T	A	A	A	G	C	T	T	C	C	T	C	C	A	C	C	C	G	G
Cas9 #31	0.0	T	100.0	0.0	0.0	99.9	99.9	0.0	0.0	0.0	0.2	0.0	99.9	97.8	0.0	0.0	99.9	0.0	0.0	0.1	1.4	0.0	0.0	0.1
		G	0.0	0.0	0.0	0.0	0.0	0.0	0.0	0.0	99.8	0.0	0.0	0.6	0.0	0.0	0.0	0.0	0.0	0.0	1.2	0.0	99.9	99.9
		C	0.0	0.1	99.9	0.0	0.0	0.0	0.0	0.0	0.0	100.0	0.0	0.1	99.9	99.9	0.1	99.9	99.0	0.0	99.8	99.6	99.9	0.0	0.1
		A	0.0	99.9	0.0	0.0	0.0	99.9	99.9	99.9	0.1	0.0	0.0	1.5	0.0	0.0	0.0	0.1	0.1	99.9	0.1	0.8	0.0	0.1
nCas9-CDA1^Hs #1	0.1	T	100.0	0.0	0.0	99.9	99.8	0.0	0.1	0.0	0.1	0.0	99.9	97.8	0.2	0.1	99.9	0.1	0.1	0.0	1.5	0.1	0.0	0.1
		G	0.0	0.0	0.0	0.0	0.0	0.0	0.1	0.1	99.8	0.0	0.0	0.5	0.0	0.0	0.0	0.0	0.0	0.0	1.3	0.0	99.9	99.8
		C	0.0	0.1	100.0	0.0	0.1	0.0	0.0	0.0	0.0	99.9	0.0	0.2	99.7	99.9	0.1	99.8	99.8	0.0	99.8	96.3	99.8	0.0	0.1
		A	0.0	99.9	0.0	0.0	0.0	99.9	99.8	99.9	0.1	0.0	0.0	1.5	0.1	0.0	0.1	0.1	0.1	99.9	0.1	0.8	0.1	0.1
nCas9-CDA1^At #3	0.1	T	99.9	0.0	0.0	100.0	99.8	0.0	0.0	0.0	0.1	0.0	99.9	98.1	0.1	0.0	99.9	0.1	0.1	0.0	1.5	0.1	0.0	0.1
		G	0.0	0.0	0.0	0.0	0.0	0.0	0.0	0.0	99.8	0.0	0.0	0.5	0.0	0.0	0.0	0.0	0.0	0.0	1.3	0.0	99.9	99.9
		C	0.0	0.1	99.9	0.0	0.1	0.0	0.1	0.0	0.0	100.0	0.1	0.1	99.8	99.9	0.0	99.8	99.8	0.0	99.8	96.5	99.8	0.0	0.1
		A	0.0	99.9	0.0	0.0	0.0	99.9	99.9	99.9	0.1	0.0	0.0	1.3	0.0	0.0	0.0	0.1	0.1	99.9	0.1	0.8	0.0	0.1
dCas9-CDA1^Hs #3	0.0	T	100.0	0.0	0.0	99.9	99.9	0.0	0.0	0.0	0.1	0.0	99.9	97.8	0.1	0.0	99.9	0.0	0.0	0.0	1.5	0.1	0.0	0.1
		G	0.0	0.0	0.0	0.0	0.0	0.0	0.0	0.0	99.8	0.0	0.0	0.6	0.0	0.0	0.0	0.0	0.0	0.0	1.3	0.0	99.9	99.8
		C	0.0	0.1	99.9	0.0	0.1	0.0	0.0	0.0	0.0	99.9	0.0	0.4	99.9	99.9	0.1	99.9	99.9	0.0	99.8	96.5	99.9	0.0	0.1
		A	0.0	99.9	0.0	0.0	0.0	99.9	99.9	99.9	0.1	0.0	0.0	1.4	0.0	0.0	0.0	0.1	0.1	99.9	0.1	0.8	0.0	0.1
nCas9 #4-2	0.1	T	100.0	0.0	0.0	99.9	99.8	0.0	0.1	0.0	0.1	0.0	99.9	97.8	0.1	0.0	99.9	0.1	0.0	0.1	1.5	0.1	0.0	0.1
		G	0.0	0.0	0.0	0.0	0.0	0.0	0.0	0.0	99.8	0.0	0.0	0.6	0.0	0.0	0.0	0.0	0.0	0.0	1.3	0.0	99.9	99.9
		C	0.0	0.1	99.9	0.0	0.2	0.0	0.0	0.0	0.0	99.9	0.0	0.2	99.9	99.9	0.1	99.9	99.8	0.0	99.8	96.3	99.9	0.0	0.0
		A	0.0	99.9	0.0	0.0	0.0	99.9	99.8	99.9	0.1	0.0	0.0	1.4	0.0	0.1	0.0	0.1	0.1	99.9	0.1	0.9	0.0	0.0
WT	0.1	T	100.0	0.0	0.0	99.9	99.9	0.0	0.1	0.0	0.1	0.0	99.9	97.8	0.1	0.0	99.9	0.0	0.0	0.1	1.6	0.1	0.0	0.1
		G	0.0	0.0	0.0	0.0	0.0	0.0	0.0	0.0	99.8	0.0	0.0	0.6	0.0	0.0	0.0	0.0	0.0	0.0	1.1	0.0	99.9	99.9
		C	0.0	0.0	100.0	0.0	0.1	0.0	0.0	0.0	0.0	100.0	0.0	0.1	99.9	99.9	0.1	99.9	99.8	0.0	99.9	96.5	99.8	0.0	0.1
		A	0.0	99.9	0.0	0.0	0.0	99.9	99.9	99.9	0.1	0.0	0.0	1.5	0.0	0.0	0.0	0.1	0.1	99.9	0.1	0.8	0.0	0.1

The ON- and OFF-target sequences of $SlDELLA^{T1}$ are indicated in bold red and mismatches in OFF-target sequences are shown in blue. T_0 transgenic plants in which each transformation vector was integrated and used for the targeted sequencing using the Mi-Seq sequencer. *Cas9* is the conventional CRISPR/Cas9 vector which induces DSB, whereas the translational fusions of *CDA1* with *nCas9* or *dCas9* are Target-AID vectors, which induce DNA substitution. The *nCas9* vector acts as a negative control owing to the presence of a stop codon in front of *CDA1*. WT is also a negative control in this experiment and its DNA was used for targeted sequencing analysis. The rate of each nucleotide (T/G/C/A) in each position on the ON- and OFF-target sites and their PAM-sequences are indicated, and the original sequences are highlighted in grey. The indels rate or the mutated nucleotide occurrence higher than 1.0% and 5.0% are highlighted in light yellow and yellow, respectively. Cas9, CRISPR associated protein 9. dCas9, dead Cas9. nCas9, nickase Cas9. CDA1, cytidine deaminase 1. [Hs], Human codon optimized. [At], Arabidopsis codon optimized.

was conducted twice independently (Table 1 and Table S4) and the representative results for each vector are presented in Table 1.

In contrast to the *Cas9*_#31 plants (numbers following # represent the names of independent line), which showed only the induction of indels with an efficiency of 46.1%, the *nCas9-CDA1^Hs*_#1 and *nCas9-CDA1^At*_#3 plants showed nucleotide substitutions, intensively occurring at the two cytidines located at the 5′-terminal region of the ON-target site, and the efficiency of the substitutions was 48.2% (C-to-T) and 50.7% (C-to-G/T, [54.4% + 3.1%]) in *nCas9-CDA1^Hs*_#1, and 30.5% (C-to-T) and 59.5% (C-to-T/G, [3.9% + 46.8%]) in *nCas9-CDA1^At*_#3 (Table 1). The nucleotide substitutions in these plants occurred predominately at the 5′-end of the sgRNA (Fig. 2a). By contrast, the *dCas9-CDA1^Hs*_#3 plants showed neither the induction of indels nor any nucleotide substitutions, which was equivalent to that of the *nCas9*_#4–2 plants— the negative control in the experiment (Table 1). In addition, all T_0 plants showed the same occurrence rate for each nucleotide (A, G, C, and T), as well as indel incidence, compared with that in wild-type (WT) plants at the OFF-target site, indicating the high target specificity (Table 1 and Table S4). After segregation, genome-edited plants with five substitution patterns,

from the WT *CAC* to *tAt/CAt/CAg/tAg/aAg* (Fig. 2b), with single or double amino acid substitutions, could be selected and used for further experiments (Fig. 2b and Fig. S2a). The *CAt* pattern reproduced the same amino acid substitution of the SlDELLA protein (L567F) as in the *procera-2* mutant [21]. Detailed information of these five amino acid substitutions in the genome-edited plants is provided in Fig. S2a.

In addition to nucleotide substitution, the Target-AID vectors also induced indels (Fig. 2a). In contrast to the *Cas9* vector that exclusively induced indels restricted to a few bases upstream of the PAM sequence, the Target-AID vectors induced indels that were located in the relative upstream position (Fig. 2a). Thus, the detailed indel spectra, including its position and length, were analyzed with the target sequencing data from the T_0 plants (Fig. 2c and d). The indel position in *Cas9* had only one peak at the 3′-terminal region of the target site, whereas two peaks occurred in the *nCas9-CDA1^Hs* and *nCas9-CDA1^At* vectors (Fig. 2c). One of indel peaks induced by the Target-AID vectors shared a similar location with that of *Cas9* (3′-terminal region of the target site), whereas another peak was located in the middle region of the target site (Fig. 2c). According to their representative indel sequence data, the 3′-terminal
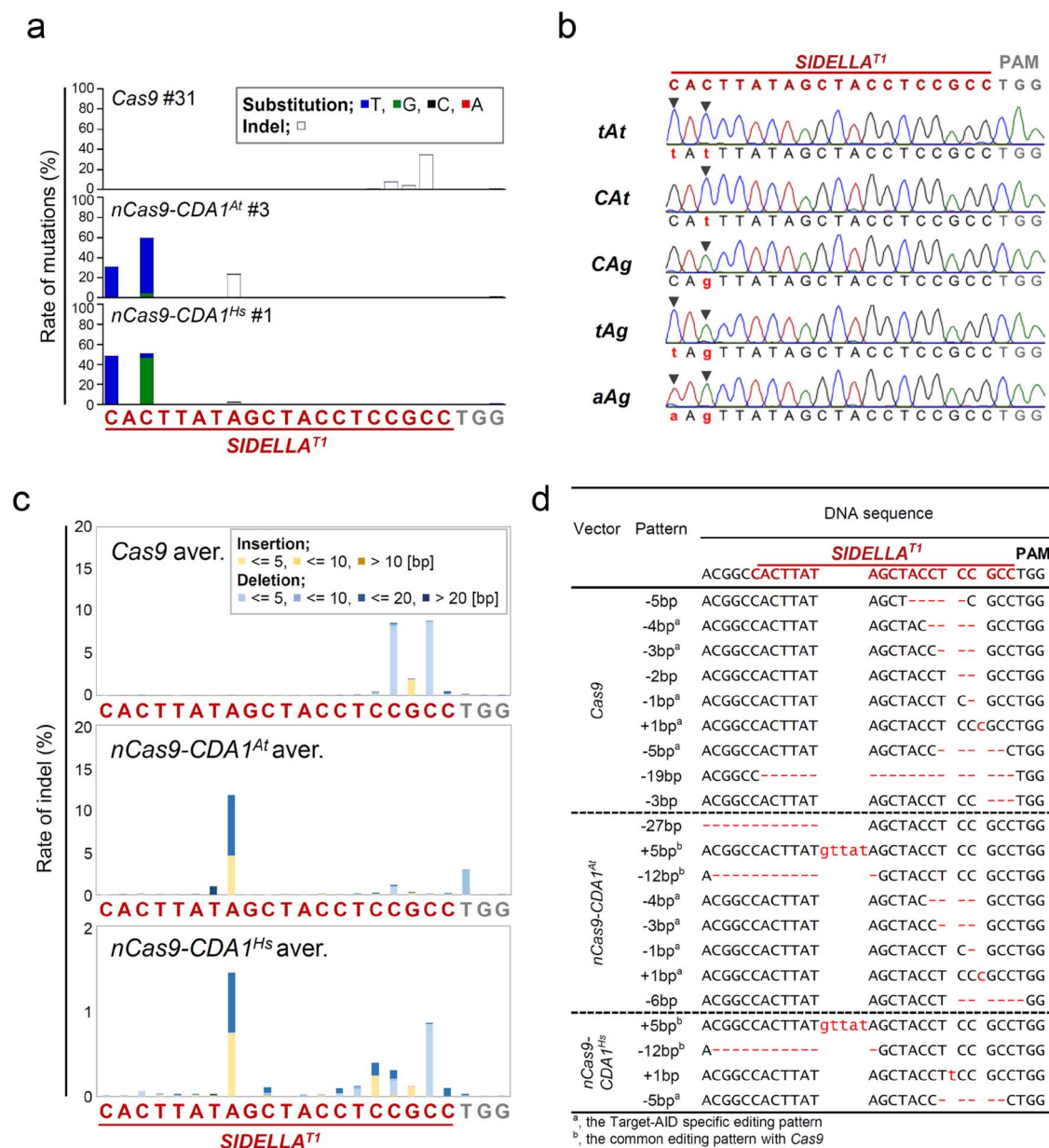
Figure 2. *SlDELLA^{T1}* targeted editing using the Target-AID system. **a** The rate of substitution and indel at each position of the target site in the representative T$_0$ plants. These frequencies are summarized results for the target sequence. **b** The nucleotide-substituted spectra in the Sanger sequence analysis of the progenies. **c** The summary of indel position and size calculated from total target sequencing data. Each frequency was averaged by the number of independent plants analyzed. The sgRNA target sequence is indicated in bold; the PAM sequence is indicated in grey; the insertions and the deletions are indicated in yellow and blue, respectively. **d** The target sequence is indicated in red bold font. The representative indel pattern had higher frequencies, which was more than 0.2%. The insertions and deletions are indicated by small red letters and dash. *Cas9*, CRISPR associated protein 9; *dCas9*, dead Cas9; *nCas9*, nickase Cas9; *CDA1*, cytidine deaminase 1; *^{Hs}*, Human codon optimized; *^{At}*, Arabidopsis codon optimized.

indel peaks shared similar editing positions among the three vectors, and the patterns of the middle indel peaks were common only in *nCas9-CDA1^{Hs}* and *nCas9-CDA1^{At}* (Fig. 2d). These results indicate that the Target-AID vectors could induce Target-AID-specific indels with editing positions different from those of the *Cas9* vectors. Moreover, indels occurred more frequently in *nCas9-CDA1^{At}* than in *nCas9-CDA1^{Hs}* (Fig. 2c). This tendency of the editing pattern was confirmed by Sanger sequencing in T$_0$ and T$_1$ plants (Tables S1–S3). The editing frequencies by Sanger sequencing for T$_0$ and T$_1$ plants were 22.8% and 22.7% in *nCas9-CDA1^{Hs}*, and 33.4% and 55.2% in *nCas9-*

CDA1^{At}, respectively (Tables S2 and S3). These results indicate that *nCas9-CDA1^{At}* and *nCas9-CDA1^{Hs}* shared the similar editing traits, but *nCas9-CDA1^{At}* was likely more efficient. This may be because of the different *CDA1-*codon usage, and *Arabidopsis* codon-optimized *CDA1^{At}* may increase the translation efficiency and thus, the number of genome-editing events in tomato cells [4, 7, 9].

Furthermore, to investigate whether *nCas9-CDA1* is able to edit different genes, we targeted *SlETR1*, which encodes the regulator of the plant hormone ethylene [25]. Four sgRNAs (*SlETR1^{T1}–SlETR1^{T4}*) were designed to target different sites on *SlETR1*; *SlETR1^{T2}* targeted the

same 20 bp sequence on both *SlETR1* and *SlETR2*. The sgRNAs were introduced into the *nCas9-CDA1*[At] and/or *Cas9* vectors (Fig. S1). All T_0 and T_1 plants showed nucleotide substitutions (C-to-T/G/A) and/or indels on three *SlETR1*-specific target sites and the *SlETR1/2* dual-gene target site (Fig. S2b). Notably, the editing spectrum showed that the *nCas9-CDA1*[At] vector could induce both indels and nucleotide substitutions in all four target sites (Fig. S2c–f). Moreover, *nCas9-CDA1*[At] vectors double targeting *SlDELLA*[T1]/*SlETR1*[T2] and *SlDELLA*[T1]/*SlHWS*[T2] were constructed to investigate the multi-target genome-editing efficiency of the Target-AID system (Fig. S1). We observed that all the T_0 and T_1 plants displayed nucleotide substitutions (C-to-T/G/A) or indels at the target site (Fig. S3a and b).

In the *SlDELLA* target, both Target and Sanger sequencing analyses revealed that the *dCas9-CDA1*[Hs] vectors barely induced nucleotide substitutions and indels unlike the *nCas9-CDA1* vectors (Table 1 and Tables S2–S4). To test if the unavailability of this vector was due to the intrinsic property of the editing protein or due to the incompatibility of the target sequence, we designed a vector that double-targeted *SlDELLA*[T1]/*SlHWS*[T1] using *dCas9-CDA1*[At] and *dCas9-CDA1*[At]*-UGI*, in "Micro-Tom" and/or a commercial parental cultivar ("UT-B"); the detailed genome-editing spectrum is shown in Fig. S3b. The "Micro-Tom" T_0 and T_1 plants showed efficient induction of both indel and nucleotide substitutions with both the vectors, only at the ON-target site of *SlHWS* but not at the ON-target site of *SlDELLA* (Fig. S3b). Interestingly, the *dCas9-CDA1*[At]*-UGI* vector targeting *SlDELLA*[T1]/*SlHWS*[T1] in the commercial parental cultivar ("UT-B") showed an induction of mutations at the ON-target site of both *SlHWS* and *SlDELLA* unlike in the "Micro-Tom" background (Table 1), indicating that the genetic background might be a factor that restricts the genome-editing efficiency, and the use of UGI may increase the genome-editing efficiency of the Target-AID system. Our results indicate that the vectors of Target-AID, *nCas9-CDA1*[Hs/At], *dCas9-CDA1*[At], and *dCas9-CDA1*[At]*-UGI* have the ability to induce not only C-to-T nucleotide substitutions but also C-to-A/G substitutions and indels, despite the inability of inactivated Cas9 to induce DSB.

Phenotype analysis of *SlDELLA*-genome-edited "micro-tom" and F_1 hybrid tomatoes

GA has been shown to regulate the internode growth, leaf shape, style length, and formation of parthenocarpic fruit in tomatoes [18, 26, 27]. To evaluate the genome-edited plants, five mutations (*tAt*, *CAt*, *CAg*, *tAg*, and *aAg*), named with the nucleotide substitution sequences (the lower case indicates the substituted base and the upper case indicates the original base), were selected and investigated together with strong GA-insensitive *procera* (*pro*) plants that harbor a point mutation in the VHIID subdomain in the GRAS domain of the SlDELLA protein [22] (Fig. S2a, Fig. 3). Among the five genome-

edited plants, the *CAt* plants displayed mutations identical to the *procera-2* mutant [21]. Subsequently, the GA-related phenotypes were analyzed in these plants. The average height of *procera* plants was 15 cm, which was higher than that of WT (10 cm) and *CAt* (14 cm) plants (Fig. 3a, b). Interestingly, one genome-edited plant, *tAt*, was the tallest at 18 cm (Fig. 3a, b). Additionally, diminished leaf serration and perturbation of the style could be observed in the *procera*, *CAt*, and *tAt* plants (Fig. 3a). These findings indicate that the GA signaling is activated the most in *tAt* plants, followed by that in *procera* and *CAt* plants; the results for *procera* and *CAt* plants were consistent with those reported previously [21]. Moreover, in contrast to the WT plants, which barely showed parthenocarpy (2.0%), the *tAt* plants showed the highest parthenocarpy rate of 59.5%, and the results of the *procera* (31.0%) and *CAt* (21.0%) plants followed the same trend as those for the other GA-related phenotypes (Fig. 3c). A clear enlargement of the ovaries in these mutants was observed at 7 days after anthesis (DAA) and after emasculation at 1 day before anthesis (-1DAA) (Fig. 3d). In contrast, plants with all other mutations (*CAg*, *tAg*, and *aAg*) showed similar growth and parthenocarpy rate compared with that in the WT plants, indicating that these mutations have no or limited effect on the GA-signaling pathway (Fig. 3a–c).

To test the applicability of the Target-AID system in commercial tomato cultivars, vectors were introduced into three commercial parental cultivars ("UT-A", "UT-B", "UT-I"); the *nCas9-CDA1*[At] vector with *SlDELLA*[T1]-targeting sgRNA was transformed into the female parental "UT-A" and "UT-B", and the male parental "UT-I" of medium-sized tomato cultivars (Fig. S4a). The mutation spectrum in the T_0 generation showed that nucleotide substitutions and indels were efficiently induced, and the substitutions predominately occurred in the 5'-terminal region of the target site (Fig. S4b). The distribution of these genome-editing patterns on the target sequence was consistent with the results obtained from the "Micro-Tom" cultivar (Fig. S4b and Fig. 2).

Plants with a variety of nonsynonymous mutations of the female parent "UT-B" and the male parent "UT-I" were selected (Fig. 4a) and eight mutations were obtained in the F_1 generation after crossing, including the *tAt* homozygote, *tAt* heterozygote with other patterns, and the *CAt*/*CAg* heterozygote mutation (Fig. 4b). The GA-related phenotypes of these plants were investigated in the greenhouse. Among them, plants with two alleles, *tAt*/*tAt* and *CAt*/*tAt*, showed GA-related phenotypes, such as an increased stem length and protuberant style (Fig. 4c). The parthenocarpy rate was defined in two standards, 14 and 21 days, which specify the limited days that an ovary needs to grow into a fruit with a diameter of 1 cm after emasculation at −1 DAA. In the 14-day standard, the *CAt*/*tAt* and *tAt*/*tAt* plants showed a parthenocarpy rate of 14.3% and 72.2%, respectively (Fig. S5). The 21-day standard increased the parthenocarpy rate to 77.1% for *CAt*/*tAt* and 94.4% for *tAt*/*tAt* (Fig. S5).
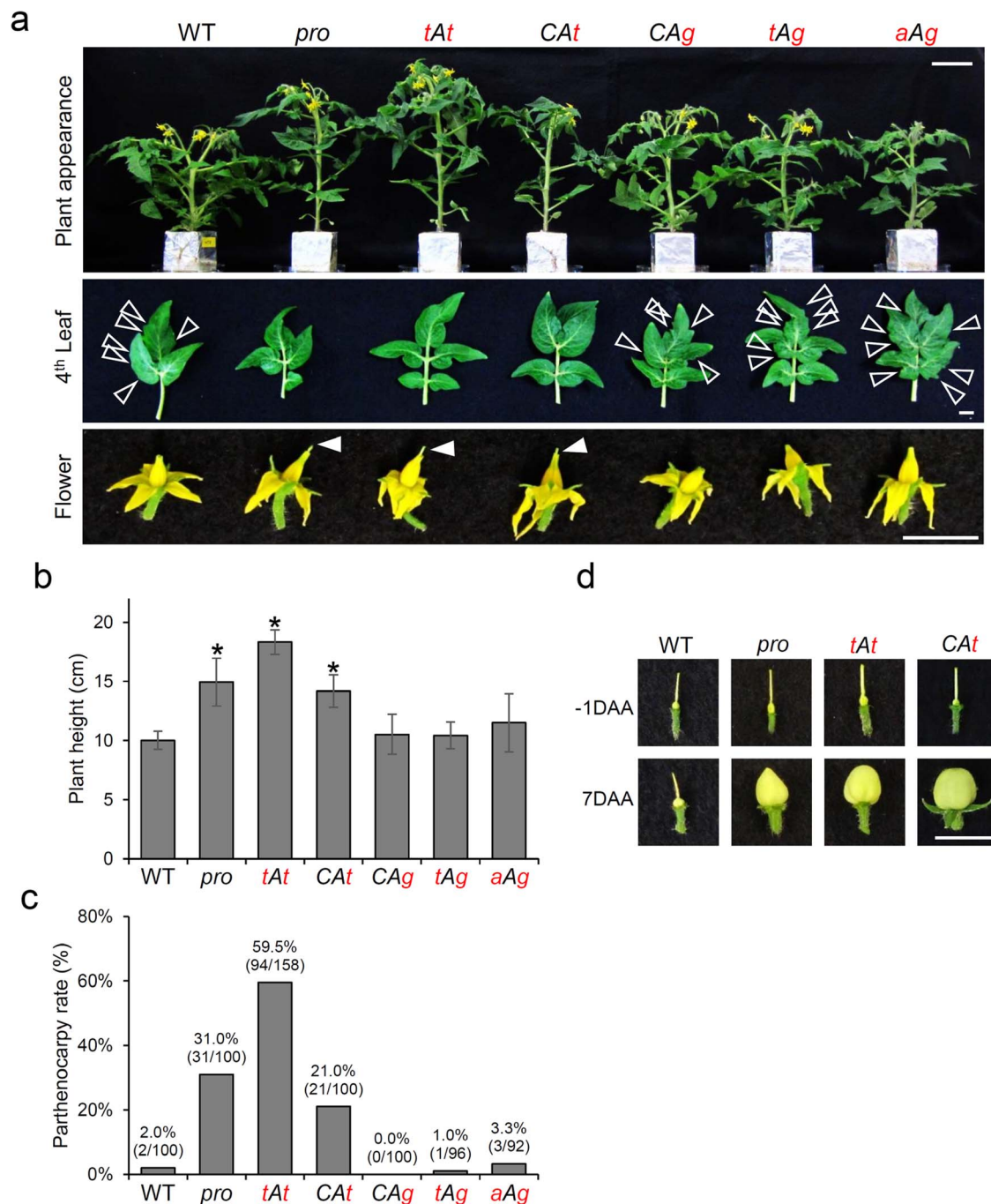
Figure 3. Phenotype analysis of the *SlDELLA*[T1] edited "Micro-Tom". **a** Photograph taken at 45 days after germination for assessment of the appearance of plants (upper) and phenotype of the 4th leaf (middle), and the flower phenotype at flowering day (lower). Bar = 5 (upper) and 1 cm (middle and lower). **b** Statistical analysis of the plant height. The plant height was measured from the base of the cotyledon to the base of the first truss. Error bar represents ± SE. Asterisks indicate significant differences compared with WT (Student's *t*-test, $p < 0.05$). **c** The parthenocarpy rate of the genome-edited plants. The numbers inside the parentheses specify the number of positive parthenocarpic ovaries versus the total number of emasculated flowers. **d** The ovary phenotype at −1 DAA, at the emasculation day, and at 7 DAA. The "Micro-Tom" *procera* mutant and WT plants were used as positive and negative controls in the phenotypic comparison, respectively. DAA, day after anthesis; bar = 1 cm; WT, wild-type; *pro*, *procera*.

In contrast, all the plants containing the other alleles showed no or limited effect on both the GA response and parthenocarpy rate compared with that in the WT plants (Fig. 4c and Fig. S5), indicating that the *tAg*, *CAa*, *GtT*, and *CAg* editing patterns had no or limited impact on the function of the SlDELLA protein, and that the heterozygosity of the *tAt* mutation did not affect GA sensitivity. These results indicated that the biological impact of the *tAt/tAt* homozygote allele is stronger than that of the *CAt/tAt* heterozygote allele, which is consistent with the results of the phenotypes of the *CAt* and *tAt* mutants in "Micro-Tom" (Fig. 3). Moreover, both the parthenocarpic and seeded fruits of the *tAt/tAt* and *CAt/tAt* plants had smaller size and lower fresh weight compared with those of the WT fruits (Fig. 4c and Fig. S5). These findings indicate that the *tAt* mutation led to a strong parthenocarpic
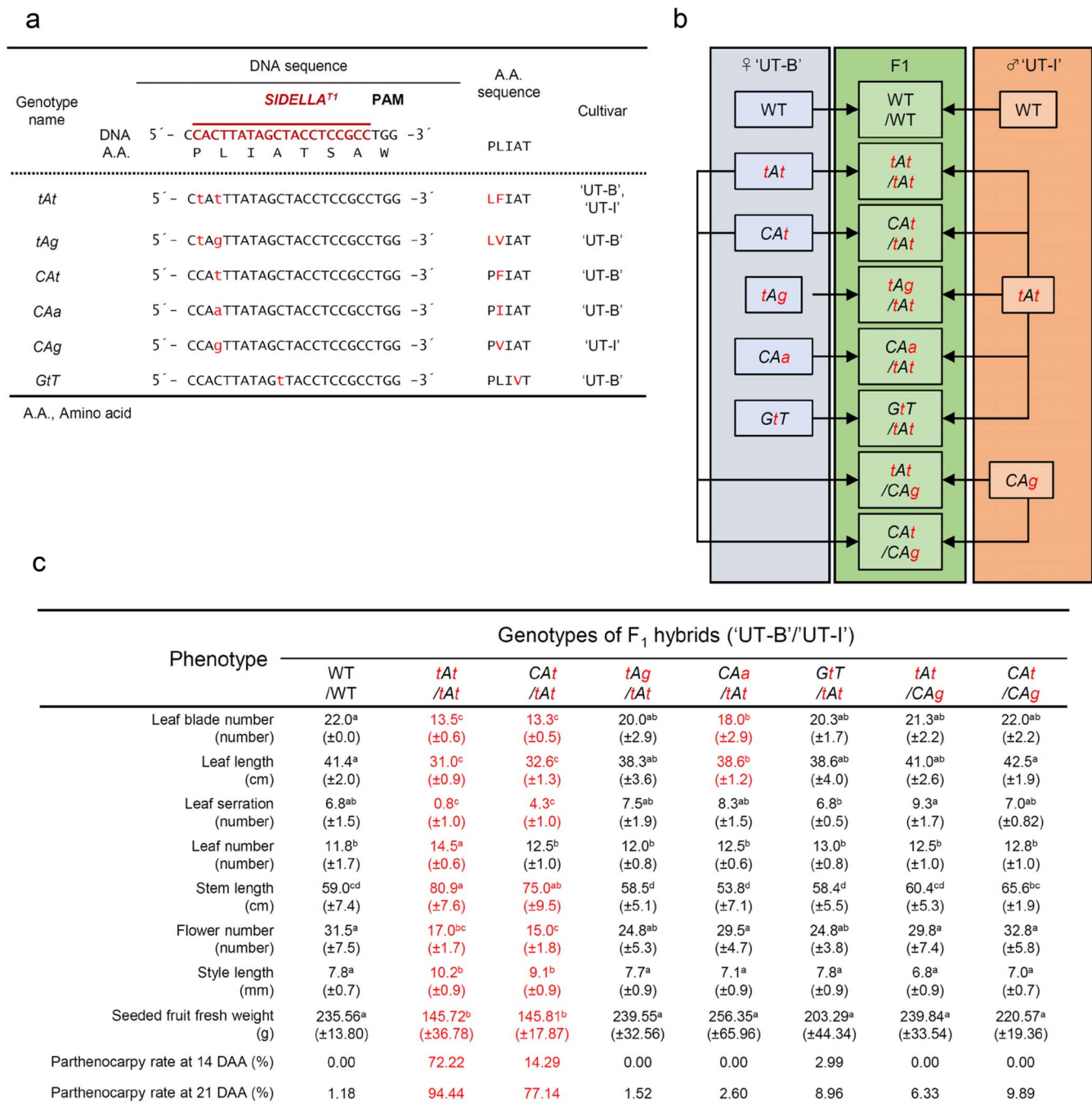
a Detailed information about the mutation in the $SlDELLA^{T1}$ edited commercial tomato cultivars ("UT-B" and "UT-I").

b Scheme of the F_1 hybrids ("UT-B"/"UT-I") of the $SlDELLA^{T1}$ edited commercial tomato cultivars.

c Phenotypic analysis of the F_1 hybrids of the $SlDELLA^{T1}$ edited tomatoes.

Phenotype	Genotypes of F_1 hybrids ('UT-B'/'UT-I')							
	WT /WT	tAt /tAt	CAt /tAt	tAg /tAt	CAa /tAt	GtT /tAt	tAt /CAg	CAt /CAg
Leaf blade number (number)	22.0[a] (±0.0)	13.5[c] (±0.6)	13.3[c] (±0.5)	20.0[ab] (±2.9)	18.0[b] (±2.9)	20.3[ab] (±1.7)	21.3[ab] (±2.2)	22.0[ab] (±2.2)
Leaf length (cm)	41.4[a] (±2.0)	31.0[c] (±0.9)	32.6[c] (±1.3)	38.3[ab] (±3.6)	38.6[b] (±1.2)	38.6[ab] (±4.0)	41.0[ab] (±2.6)	42.5[a] (±1.9)
Leaf serration (number)	6.8[ab] (±1.5)	0.8[c] (±1.0)	4.3[c] (±1.0)	7.5[ab] (±1.9)	8.3[ab] (±1.5)	6.8[b] (±0.5)	9.3[a] (±1.7)	7.0[ab] (±0.82)
Leaf number (number)	11.8[b] (±1.7)	14.5[a] (±0.6)	12.5[b] (±1.0)	12.0[b] (±0.8)	12.5[b] (±0.6)	13.0[b] (±0.8)	12.5[b] (±1.0)	12.8[b] (±1.0)
Stem length (cm)	59.0[cd] (±7.4)	80.9[a] (±7.6)	75.0[ab] (±9.5)	58.5[d] (±5.1)	53.8[d] (±7.1)	58.4[d] (±5.5)	60.4[cd] (±5.3)	65.6[bc] (±1.9)
Flower number (number)	31.5[a] (±7.5)	17.0[bc] (±1.7)	15.0[c] (±1.8)	24.8[ab] (±5.3)	29.5[a] (±4.7)	24.8[ab] (±3.8)	29.8[a] (±7.4)	32.8[a] (±5.8)
Style length (mm)	7.8[a] (±0.7)	10.2[b] (±0.9)	9.1[b] (±0.9)	7.7[a] (±0.9)	7.1[a] (±0.9)	7.8[a] (±0.9)	6.8[a] (±0.9)	7.0[a] (±0.7)
Seeded fruit fresh weight (g)	235.56[a] (±13.80)	145.72[b] (±36.78)	145.81[b] (±17.87)	239.55[a] (±32.56)	256.35[a] (±65.96)	203.29[a] (±44.34)	239.84[a] (±33.54)	220.57[a] (±19.36)
Parthenocarpy rate at 14 DAA (%)	0.00	72.22	14.29	0.00	0.00	2.99	0.00	0.00
Parthenocarpy rate at 21 DAA (%)	1.18	94.44	77.14	1.52	2.60	8.96	6.33	9.89

Figure 4. $SlDELLA^{T1}$ editing in the commercial cultivars. **a** Detailed information about the mutation in the $SlDELLA^{T1}$ edited commercial tomato cultivars ("UT-B" and "UT-I"). **b** Scheme of the F_1 hybrids ("UT-B"/"UT-I") of the $SlDELLA^{T1}$ edited commercial tomato cultivars. **c** Phenotypic analysis of the F_1 hybrids of the $SlDELLA^{T1}$ edited tomatoes. Leaf blade number, leaf length, and leaf serration were determined for the leaf under the 1st truss at the time of flowering of the first flower. The leaf number and stem length were determined from the cotyledon to the 1st truss. Flower number was counted in the 2nd, 3rd, and 4th truss. Style length was measured for all flowers. Seeded fruit was assessed using the 1st truss of each plant, with three fruits per truss; the weight was measured at the breaker stage. Numbers in parenthesis indicate error bars represented by ±SE. Letters indicate significant differences (Student's t-test, $p < 0.05$). N > 30, except for seeded fruit phenotype, for which N = 12. Parthenocarpy was determined by the size of ovaries that were over 1 cm at 14 or 21 DAA after the removal of stigma at −1 DAA from the 2nd truss to the 4th truss without flower limitation. The parthenocarpy rate is indicated by the quotient of the number of parthenocarpy fruit and the total number of stigma removed flower bud from four plants of each genotype. The first truss was used for evaluating the quality of the pollinated fruit with three fruits limiting manner. ♀, seed parent. ♂, pollen parent. DAA, day after anthesis. Nucleotide or amino acid substitutions were marked in red. The data showed significant difference compared with WT were shown in red.

phenotype due to the strongly activated GA-signaling pathway, which indicated that the tAt mutation severely affected the function of the SlDELLA protein.

The GRAS domain of the DELLA protein consists of LHR1, VHIID, LHR2, PFYRE, and SAW subdomains. These subdomains construct the extended Rossmann fold $\alpha/\beta/\alpha$ sandwiched conformation that contributes to the core structure of the GRAS domain, which may play an important role in protein–protein interaction [28, 29]. The 3D-structure of the GRAS family protein

domain has been elucidated for the rice OsSCL7 protein [28]. The alignment analysis against the OsSCL7 with SlDELLA protein indicated that the *procera* (SlDELLA^{V302E}) and *procera-2* (SlDELLA^{L567F}) mutants possess single amino acid substitutions occurring at the B1 β-strand of the VHIID subdomain and the B9 β-strand of the VHIID subdomain and the SAW subdomain, respectively (Fig. S6a). Moreover, given that the proline (P566) and leucine (L567) residues of SlDELLA are highly conserved in *Arabidopsis*, rice, and tomato DELLA proteins (Fig. S6b), the double amino acid substitution (SlDELLA$^{P566L/L567F}$) in *tAt* plants may severely impact the core structure of the GRAS domain, thus affecting the function of the SlDELLA protein. This may explain the stronger phenotype of the *tAt* mutant plants than that of the *procera-2* (CAt) and *procera* mutants. Thus, the Target-AID system provides a good strategy to generate mild mutants that fulfill the needs of tomato production, as well as to discover new regulatory sites that are essential for the function of the SlDELLA protein.

Phenotype analysis of *SlETR* genome-edited "micro-tom" and F$_1$ hybrid tomatoes

In addition to *SlDELLA*, we also targeted *SlETR1* with the Target-AID system. The *ETR* genes encode the receptor for the plant hormone ethylene, which regulates a variety of plant developmental processes throughout the life span of the plant, including germination, seedling growth, fruit ripening, senescence, and abscission [30, 31]. The ETR proteins are composed of an N-terminal transmembrane ethylene-binding domain (EBD) with three helices and a C-terminal cytosolic signaling transmitter domain. The ETR proteins negatively regulate ethylene signal transduction, and the inhibitory function of ETR is suppressed by the binding of ethylene to ETR via the N-terminal ethylene-binding domain [32]. In contrast to the five ETR members in *Arabidopsis*, the tomato genome possesses six *SlETR* genes [25, 33]. Among the six tomato SlETR members, SlETR1 and SlETR2 share around 80% sequence identity and 90% sequence similarity with the *Arabidopsis* homolog, AtETR1, respectively [23]. We have previously reported on two tomato mutants generated by EMS mutagenesis, *Sletr1–1* and *Sletr1–2*, which showed distinct strengths of ethylene-insensitive phenotypes, including delayed fruit ripening and prolonged fruit shelf life. The mutation in *Sletr1–1* and *Sletr1–2* occurred at the EBD, affecting the ethylene-binding ability of SlETR1 and resulted in a dominant insensitivity to ethylene [25]. Therefore, we targeted the EBD domain for genome-editing and examined the effect of mutations on ethylene sensitivity. As a result, four *SlETR1* targets induced a variety of nucleotide substitutions in the EBD region in "Micro-Tom" (Fig. 1a and Fig. S2c–f). Two nonsynonymous nucleotide substitutions (L54F and V58I) induced in the *SlETR1^{T4}* site were named "*c*" (L54F) and "*a*" (V58I). Plants with a single "*c*" (L54F) or a double "*ca*" (L54F and V58I) type mutation that translated single or double amino

acid-substituted SlETR1 were selected to evaluate the effect of these mutations on ethylene signaling (Fig. 5a and Fig. S2e).

The ethylene signaling-dependent triple response was examined in the presence of 10 ppm ethylene, and the *Sletr1–2* mutant plants were used as an ethylene-insensitive control (Fig. 5b and c). In contrast to the *Sletr1–2* control plants, which showed longer hypocotyls (29.1 mm) compared with those of WT (13.7 mm), the "*c*" and "*ca*" mutant plants showed shorter hypocotyls (21.0 mm for "*c*" and 22.2 mm for "*ca*" mutant plants) (Fig. 5b and c). However, the WT plants and the "*c*" and "*ca*" mutant plants displayed a normal shelf life, whereas the *Sletr1–2* plants showed a prolonged shelf life (Fig. 5d). These results indicate that the novel point mutations, "*c*" and "*ca*", produced a mild ethylene-insensitive phenotype compared with the ethylene sensitivity of the *Sletr1–2* plants (Fig. 5b–d).

Next, to investigate the possibility of genome-editing of *SlETR1* using the Target-AID system in the commercial cultivars, the same strategy was also applied to *SlETR1* with the female parents "UT-A", "UT-B", "UT-Y", and the male parent "UT-I", employing three sgRNAs: *SlETR1^{T1}*, *SlETR1^{T3}*, and *SlETR1^{T4}* (Fig. 1a and Fig. S1). The mutation spectra in the T$_0$ generation showed that nucleotide substitutions and indels were efficiently induced (Fig. S4c–e) and the positions of the substitutions were dependent on the sgRNA target sites, but they were almost always located in the anterior region of the sgRNA sequences (Fig. S4c–e). These results indicated that all three sgRNAs efficiently edited *SlETR1* in both the parental tomato cultivars.

The same single "*a*" and double "*ca*" mutations at the *SlETR1^{T4}* site were selected from the female parent "UT-A" and the male parent "UT-I" (Figs. S4e and S7a). After generation by crossing, the F$_1$ generation, including the *ca*/WT heterozygote, *ca*/*ca* homozygote, and *ca*/*a* bi-allele plants, was investigated in the greenhouse (Fig. S7b). Plants with these three alleles showed delayed petal senescence and fruit ripening (Fig. S7c and d). In contrast to the WT plants, which needed 67.3 days from flowering to reach the breaker stage, the *ca*/*ca* and *ca*/WT plants required 72.5 days and 69.2 days from flowering to the breaker stage, respectively (Fig. S7d). The *ca*/*a* plants were associated with faster fruit ripening compared with *ca*/*ca* plants, but the ripening was delayed compared with that of *ca*/WT plants (Fig. S7d). These findings indicate that the double point mutation affected the function of SlETR1 protein more strongly than did the single point mutation. Moreover, corroborating the results of the experiment with "Micro-Tom" (Fig. S6d), the shelf life was not affected by the F$_1$ hybrid ("UT-A"/"UT-I") alleles (Fig. S7e and f).

The "*c*"-type and "*a*"-type mutations of SlETR1 in the genome-edited tomatoes occurred at L54 and V58, corresponding to the amino acids L39 and V43 of the *Arabidopsis* homolog AtETR1, respectively (Fig. 5, Fig. S7). The L39 of AtETR1 plays an essential role in the ethylene
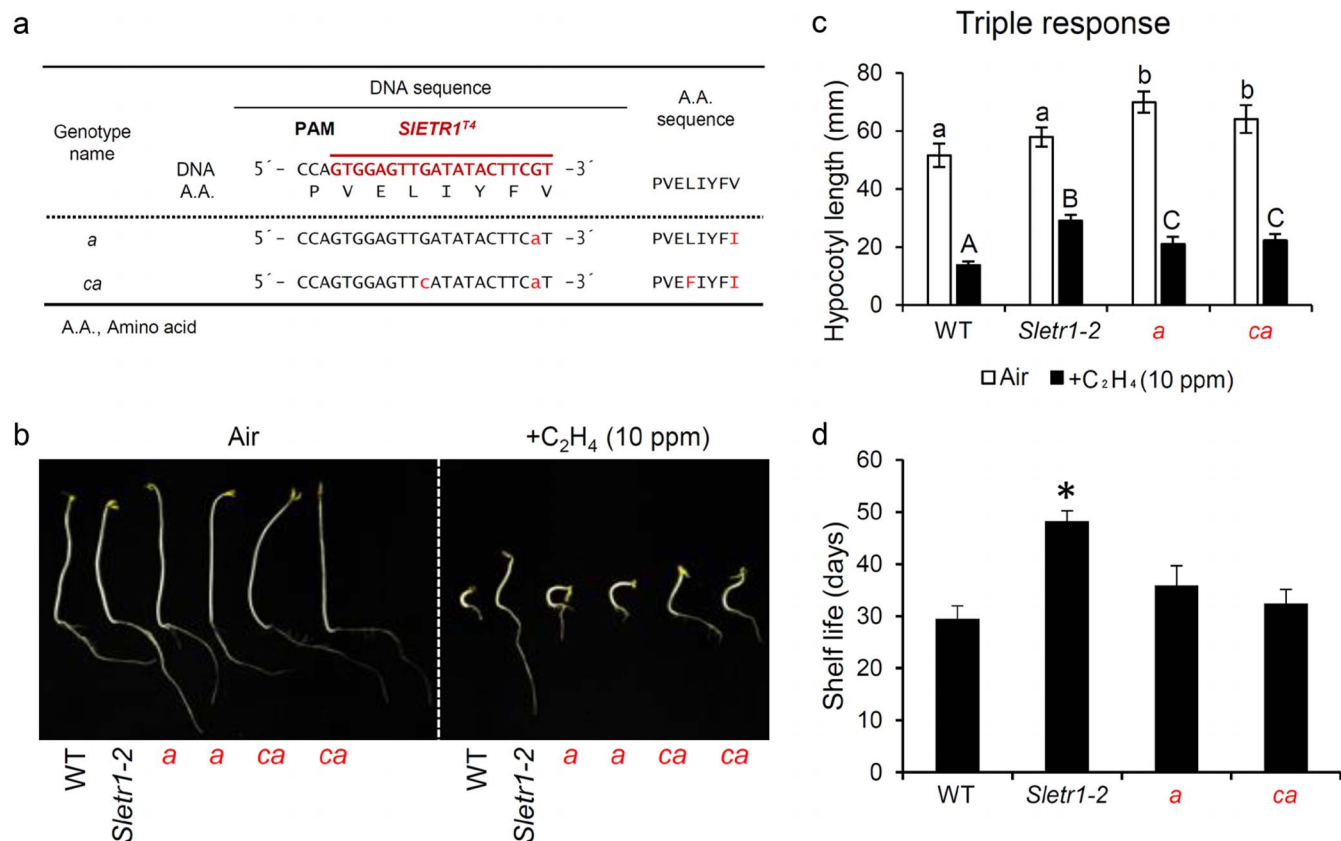
Figure 5. Phenotype of $SlETR1^{T4}$ genome-edited "Micro-Tom" plants. **a** Detailed information about the mutations in the $SlETR1^{T4}$ edited "Micro-Tom". **b** Triple response. Ethylene was applied 2 days after sowing, and the photograph was taken 5 days after the treatment. The experiment was conducted with 10 repetitions, and a representative picture is shown. **c** Quantitative data for the result presented in **b**. **d** Shelf life. Fruits were harvested 7 days after the breaker stage. Shelf life was evaluated under room conditions (25°C) until wrinkling appeared on the fruit surface (N > 7). Asterisks indicate significant differences compared with WT (Student's *t*-test, $p < 0.05$).

binding of the EBD, whereas the V43 has not been shown to have an essential function. However, the adjacent F42 amino acid seems to regulate the signal transmission of AtETR1 [34]. The more delayed fruit ripening in the *ca/a* plants compared with that in the *ca*/WT plants might be due to the hindrance of the adjacent functional site by the presence of the "*a*"-type mutation. In addition, unlike the "Micro-Tom", the *Sletr1–1* mutant showed incomplete ripening [25], and the plants with "*ca*" or "*a*" mutation in the F_1 hybrids ("UT-A"/"UT-I") showed prolonged fruit ripening (Fig. S7d). The mutation site of *Sletr1–1* corresponds to the P36 of AtETR1, which reduced the ethylene-binding activity of AtETR1 to 5%, whereas the "*c*"-type mutation in the genome-edited tomatoes corresponds to the L39 of AtETR1 and the substitution of this site reduced the ethylene-binding activity of AtETR1 to 60% [34]. These results suggest that the "*c*" mutation induced a milder phenotype compared with that in the *Sletr1–1* mutant. This could explain the delayed, but complete, ripening of "*c*" mutation plants. The normal shelf life of these mutants might be due to the weak effect on ethylene signaling compared with that in the *Sletr1–2* mutant.

In this study, by targeting *SlDELLA*, we could obtain a variety of genome-editing patterns with single or double amino acid substitutions and isolated the *tAt* mutant plants exhibiting strong parthenocarpy phenotypes in

both the model "Micro-Tom" and "UT-B", and F_1 hybrid ("UT-B"/"UT-I") (Figs. 3, 4 and Fig. S5). Together with the result of *SlETR1* targeting, double targeting, and multi-sgRNA targeting in both "Micro-Tom" and F_1 hybrid ("UT-A"/"UT-I"), we demonstrate the versatility of the Target-AID system in tomato genome-editing (Fig. 5 and Fig. S7).

A model of Indel induction by Target-AID in tomato

CDA1 generally catalyzes the deamination reaction of cytidine (C) and initially produces uridine (U), which is expected to be replaced by T in the subsequent DNA replication [7]. However, in *nCas9-CDA1*-induced genome editing, cytidines on the 5′-terminal region of non-complementary strand were substituted with T, G, and A (Fig. 2a and b, 5a, Figs. S2–S4 and Tables S2–S4).

Besides, indels were unexpectedly induced by *nCas9-CDA1* in the 5′-terminal region of the sgRNA, which was overlapping the nucleotide-substituted sites and was distinct with the Cas9 induced indels (Fig. 2c and d). These characteristics in *nCas9-CDA1* can possibly be explained by the involvement of base excision repair (BER) system, which fixes damaged DNA [35, 36]. If BER is involved, it likely occurs after the induction of C to U transition on non-complementary strand and

single strand break (SSB) on the complementary strand by *nCas9-CDA1*, and the U:G pair is substituted by thymidine after DNA replication, which generates C-to-T substitution (Fig. 6b). Alternatively, the mutated U:G pair could be recognized by uracil-DNA glycosylase, which removes U and generates an apurinic/apyrimidinic (AP) site with a sugar-phosphate backbone [36–38] (Fig. 6c). There are two hypotheses that can account for the generation of such unexpected mutation spectra. The first hypothesis is that translesion DNA synthesis (TLS) polymerase (synthesizes DNA strands, including the damaged base) may induce random insertion of any base into the AP site, resulting in C-to-T/G/A substitutions (Fig. 6d). The second hypothesis is that the AP site is, then, eliminated by AP lyase or AP endonuclease, which generates AP-eliminate site (the loss of nucleotide) (Fig. 6e). In this scenario, the AP-eliminated site on the non-complementary strand, together with a nick on the complementary strand induced by *nCas9*, causes extensive indels by these two lesions [35, 39]. Similar results were obtained for *dCas9-CDA1-UGI* plants, as the editing spectrum of the *SlHWS*-targeting *dCas9-CDA1*^At^-*UGI* vector showed C-to-T/G nucleotide substitutions mainly on the non-complementary strand, and the indels could be detected at the anterior of the target site (Fig. S3b), despite the dCas9 inability of inducing DNA breaks (Fig. S6). Therefore, this system might cooperate with BER during DNA replication as a result of the formation of a U:G pair by the CDA1 enzyme, and this could be linked to the generation of a variety of mutations [6].

In summary, we demonstrate that the Target-AID system could efficiently edit sgRNA-targeting sites. We were able to select a series of mutants that showed distinct agricultural traits (Figs. 3 and 5, and Figs. S5 and S7). Among the vectors tested, *nCas9-CDA*^At^ showed the highest genome-editing efficiency, likely due to codon optimization of CDA to dicot plants, whereas the effectiveness of *UGI* and 2A peptide may be limited in tomatoes considering the fact that the editing efficiency did not differ among the tested Target-AID vectors (Table S2 and Table S4). Furthermore, we show that the successful induction of nucleotide substitution via multi-targeting by a single sgRNA, and multi-targeting by multiple sgRNAs in one vector (Fig. 5 and Figs. S2–4 and S7). Besides, the Target-AID system also produced a Target-AID-specific pattern of indels (Fig. 2), and genetic background influenced the feasibility of *dCas9-CDA* as a base-editing tool (Tables S1–S4). Importantly, our results can facilitate a case study on the application of base-editing technology to translational research that aims at commercialization of genome-edited crops.

Materials and methods
Plant growth
Tomato "Micro-Tom" and four varieties of commercial parental cultivars ("UT-A", "UT-B", "UT-I", "UT-Y"), were used. Their seeds were obtained from the National Bioresource Project and a private company, respectively. Tomato seeds were imbibed on wet filter paper and germinated at 25°C. The seedlings were then transplanted to soaked rock wool (Grodum). "Micro-Tom" plants were grown in the cultivation room at 25°C under 200 μmol m^{-2} s^{-1} light intensity and 16:8 h L:D photoperiod and irrigated with a mixture of the standard nutrient solutions, OAT-1 and OAT-2 (Otsuka Chemical Co. Ltd., Osaka, Japan). The commercial cultivars were transferred to the greenhouse (>15°C) after acclimation and were irrigated with a mixture of the standard nutrient solutions, OAT-S1 and OAT-2 (Otsuka Chemical Co. Ltd.), maintaining pH in the range of 5.0–6.5. The crossing of "UT-A" or "UT-B" and "UT-I" for F$_1$ seeds and evaluation of parthenocarpy rate in *Sldella* mutants was conducted during the spring–summer period of 2018 in Tsukuba, Japan. The phenotype of the F$_1$ hybrid plants ("UT-B"/"UT-I" for *SlDELLA*-edited plants and "UT-A"/"UT-I" for *SlETR1*-edited plants) was evaluated using during the autumn–winter period of 2018 in Tsukuba, Japan.

Vector construction
The CRISPR/Cas9 vectors, *pZK_FFCas9* (*Arabidopsis* codon-optimized Cas9), *pUC19_AtU6oligo* originated from *pCAS9-TPC*, and *pChimera* [40], were kindly provided by Dr. Masaki Endo, National Institute of Agrobiological Sciences, Japan. D10A mutation in *nCas9* and D10A H840A mutations in *dCas9* were introduced in *pZK_FFCas9* by PCR (Table S6) and the vector was circularized using the Gibson assembly method. Human and *Arabidopsis* codon-optimized *CDA1s* and *UGI* were synthesized by Eurofins Genomics (Tokyo, Japan).

The vectors were constructed following the previously described protocol [12] with minor modifications. The sequence encoding a linker peptide^type1^ composed of the nuclear localized signal *SV40* (*NLS*), a glycine-serine rich peptide linker, an *SH3* domain with 3× *FLAG* tags, and human codon-optimized *CDA1* was inserted downstream of *nCas9* and *dCas9* in the *nCas9-CDA1*^Hs^ and *dCas9-CDA1*^Hs^ vectors, respectively. *nCas9-stop-CDA1*^Hs^ was digested at the linker peptide^type1^ and self-ligated to generate a stop codon. In contrast, in the *nCas9-CDA1*^Hs^, *nCas9-CDA1*^At^, and *dCas9-CDA1*^At^ vectors, the sequence encoding a linker peptide^type2^ composed of the *Arabidopsis* codon-optimized *SH3* domain with 3× *FLAG* tags was inserted as described above. The sequences for all the CDAs possessed an NLS at the 3′-terminus, which was inserted between the *Cas9* and *Pea3A* terminator sequences. In the *dCas9-CDA1*^At^-*UGI* vector, the linker peptide^type2^, *CDA1*^At^, and *UGI* were inserted in the 3′-terminus of *dCas9*. Additionally, *nCas9-CDA1*^At^-*2A* and *dCas9-CDA1*^At^-*UGI*, for the double sgRNA targeting vectors, received an NLS and IV2 intron [40] insertion at the *EcoRI* site located in the 5′-terminus of *nCas9* or *dCas9*. Moreover, to generate the modified *Cas9-2Apeptide-NPTII* vector for coexpression, *nCas9-CDA1*^At^-*2A* was digested at *ApaI*, located between the *CDA1*^At^ and
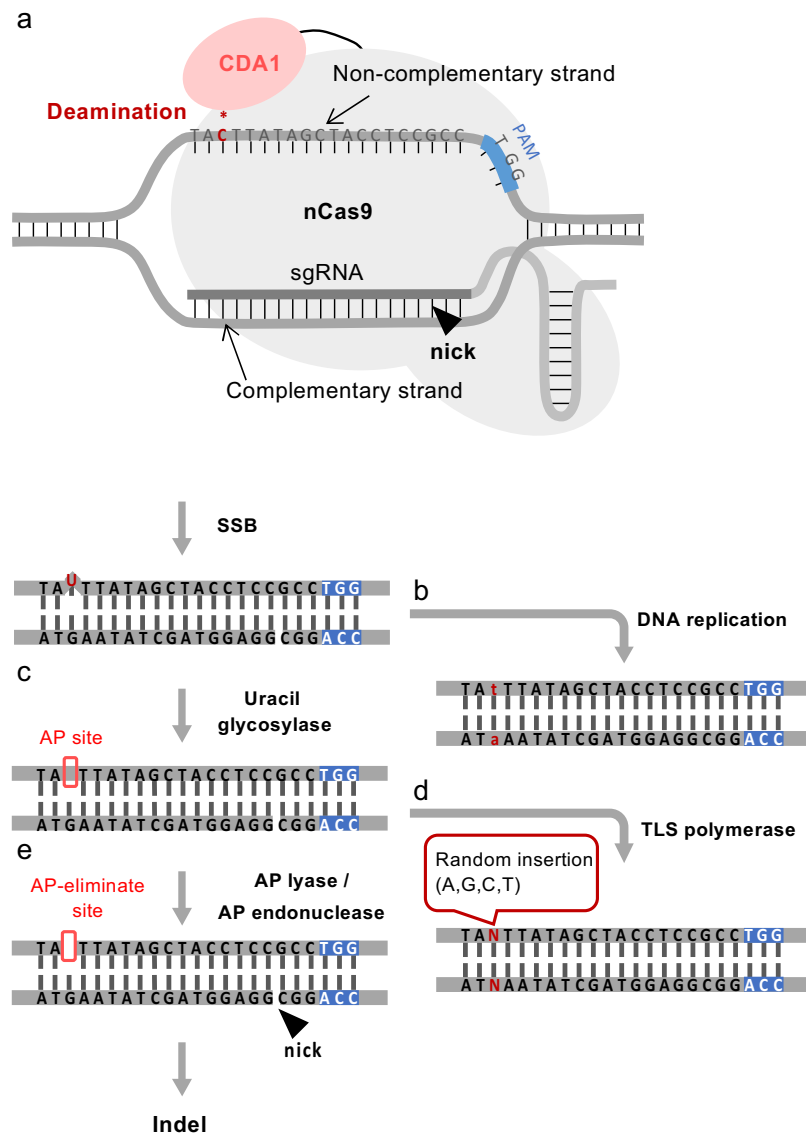
Figure 6. A model of nucleotide substitution mechanism induced by *nCas9*-based Target-AID. **a** The nCas9-CDA1 fusion protein deaminates a cytidine on the non-complementary strand and induces a nick on the complementary strand through SSB. **b** After DNA replication without DNA repair, uridine (U), cytidine-deaminated product, is substituted for thymidine **c** or the U:G pair is recognized by the uracil glycosylase and an AP site is produced. **d** Thereafter, a base is incorporated randomly at the AP site by TLS polymerase, resulting as the random nucleotide substitution. **e** Alternatively, the AP site is eliminated by AP lyase or AP endonuclease. The AP-eliminate site and a nick form SSB and induce indels. nCas9, nickase Cas9; CDA1, cytidine deaminase; AP, apyrimidinic site; TLS, translesion DNA synthesis; SSB, single strand brake; Indel, insertion and deletion.

Pea3A terminator, and the *Xba*I site, located between the *CaMV35S* promoter and *NPTII*, followed by the insertion of the sequence encoding the 2A peptide (a foot-and-mouth disease virus 2A peptide [11]) by annealing the two oligonucleotides (Table S5). The sequences of the *dCas9-CDA1^At^-UGI* and *nCas9-CDA1^At^-2A* vector are shown in Table S5. The plasmid vectors for *nCas9-CDA1^At^* and *nCas9-CDA1^At^-2A* have been deposited to Addgene (https://www.addgene.org) under the accession #91694 and #91695, respectively. The other vectors are available upon reasonable request.

We selected multitarget sites: *SlDELLA^target^*, *SlETR1^T1^*, *SlETR1/ETR2^T2^*, *SlETR1^T3^*, *SlETR1^T4^*, *SlHWS^T1^*, and *SlHWS^T2^* from *SlDELLA* (*Solyc11g011260*), *SlETR1* (*Solyc12g011330*), *SlETR2* (*Solyc07g056580*), and *SlHWS* (*Solyc01g095370*).

Each target site was inserted into *pUC19_AtU6oligo* between the *AtU6* promoter and a chimeric sgRNA scaffold by the PCR method and circularized via the Gibson assembly. For double sgRNA targeting, *SlDELLA^T1^* was combined with *SlETR1^T2^*, *SlHWS^T1^*, or *SlHWS^T2^*. *pUC19_AtU6oligo* had *Asc*I and *Spe*I sites at the 5'- and 3'-terminal regions of the AtU6 promoter-gRNA scaffold, respectively. The *Mlu*I site was inserted between the 3'-terminal region of the gRNA and *Spe*I site. Fractions including each gRNA were double-digested at the *Mlu*I-*Spe*I or *Asc*I-*Spe*I sites and the two sgRNA expression units were connected tandemly. The sgRNA expression units for the single sgRNA and the double sgRNAs were digested at two I-*Sce*I sites located in the outside region and were individually inserted into each of the modified

Cas9 vectors. The sequences of vectors used in this study are shown in Table S5.

Transformation of tomato

Each construct was introduced into the *Agrobacterium strain* GV2260, and tomato plants ("Micro-Tom" and the commercial parental cultivars) were transformed by the Agrobacterium-mediated method as described preiously [41]. The diploid plants were selected after ploidy analysis, and the transgenes were detected by the amplification of *NPTII* by PCR. The transgenic plants were grown in the cultivation room or in the green house.

Among the transgenic genome-edited plants, lines #2, #21, #26, and #31 for *SlDELLA*-targeting *Cas9*, #1, lines #5, #9, and #10 for *SlDELLA*-targeting *nCas9-CDA1^{Ht},* lines #1, #2, #3, and #27 for *SlDELLA*-targeting *nCas9-CDA1At*, lines #4–2, #5–3, #6–2, #7, #8, #9, #10, #11–2, and #12 for *SlDELLA*-targeting *nCas9-stop-CDA1*, were previously created [10] and used for sequencing analysis in this study (Fig. S2, Table S3 and S4).

Sanger sequence analysis

The DNA of the T_0 plants and their progenies was extracted from the tomato leaves. Each target was amplified by PCR using target-specific primer sets (Table S6). The PCR products were cloned into the pGEM-T easy vector (Promega, Madison, WI, USA) after joining the polyA tail and then transformed into *E. coli.* (DH5α competent cells, TaKaRa, Shiga, Japan). DNA from the *E. coli* clones was extracted, and each target was amplified again by PCR using target-specific primer sets (Table S6). The nucleotide sequence was analyzed using the Sanger sequencing service from Eurofins Genomics (https://www.eurofinsgenomics.jp). The plants other than those of the T_0 generation were subjected to Sanger sequencing directly after PCR without transformation of the clones.

Target sequence

For the OFF-target site of *SlDELLA^{T1}*, the site with four mismatches to the *SlDELLA^{T1}* targeting sequence was used as described previously [12]. In both sites of the ON- and OFF-target, following the protocol from Illumina (https://jp.illumina.com/content/dam/illumina-marketing/apac/japan/documents/pdf/2013_illumina_techsupport_session17.pdf), samples which contained ~300 bp with each target site were amplified from the genomic DNA extracted from the leaves and fused to the sequences P5-i5-R1SP and P7-i7-R2SP at the 5′- and 3′-terminus, respectively. The adaptors, i5 and i7, were used for A501–508 and A701–712, respectively, and each sample was labeled using a different adaptor combination in each T_0 plant (https://dnatech.genomecenter.ucdavis.edu/wp-content/uploads/2013/06/illumina-adapter-sequences_1000000002694-00.pdf). The NGS analysis (300 bp read length, pair-end) was repeatedly performed using Mi-Seq (Illumina) in duplicate for different T_0 plants (the results of first NGS analysis are

shown in Table 1 and Table S4 upper part, whereas those of second NGS analysis are shown in Table S4 lower part).

The raw sequence reads were trimmed with Trimomatic (Usadel Lab), with the parameters of LEADING: 10, TRAILING: 10, SLIDINGWINDOW: 4:15, and MINLEN: 51. The trimmed reads were used for mapping onto the reference sequence for both ON-target and OFF-target sequences by BWA-MEM with default settings, producing BAM files. The BAM files were sorted and indexed by Samtools, and SNPs/indels were called via a Samtools-BCFtools pipeline. The resulting VCF file was used for producing the read numbers associated with these mismatches by bam-readcount, whereas the patterns of indels were examined using igvtools.

Phenotypic analysis

For the *SlDELLA^{T1}* edited "Micro-Tom" plants, the plant height, leaf shape, and flower number were recorded at 45 days after germination. Plant height was measured as the length from the cotyledon to the base of the first truss. Parthenocarpy was determined by the size of ovaries that were over 2 mm at 7 DAA after being emasculated at −1 DAA under one flower per truss, and ten flowers per plant.

For the *SlETR1^{T4}* edited "Micro-Tom" plants, a triple response assay was conducted by sowing surface-sterilized seeds on 1/2 Murashige and Skoog medium in a sealed container and applying ethylene at a concentration of 10 ppm 2 days later. Seedlings were grown in the dark at 25°C for 5 days, after which the hypocotyl length was measured. Fruit ripening was determined by counting the number of days from anthesis to the breaker stage. Fruit shelf life was evaluated at room temperature (25°C) by counting the number of days after harvest (at 7 days after the breaker stage) until wrinkles appeared on the fruit surface.

For the *SlDELLA^{T1}* edited commercial cultivars, the phenotypes of the leaf and stem were recorded at the time of the blossom of the first flower of the second truss, and the stem length was measured as the length from the cotyledon to the base of the first truss. The length of the style was measured at −1 DAA. Parthenocarpy was determined by the size of ovaries that were over 1 cm at 14 or 21 DAA after the removal of stigma at −1 DAA from the second truss without flower limitation. The first three confirmed parthenocarpic fruits were further grown for phenotypic analysis. The first truss was used for evaluating the quality of the pollinated fruit (limited to three fruits on the truss) and the seeded fruit weight was measured at the breaker stage.

For the *SlETR1^{T4}* edited F_1 hybrids, fruit ripening was determined by counting the number of days from anthesis to the breaker stage. Shelf life was evaluated using fruits that were harvested 5 days after the breaker stage by counting the number of days until wrinkles appeared on the fruit surface under room temperature conditions (25°C).

Author contribution

HE and TA conceived the project. SK, YL, MT, HK, and LHTM generated genome-edited plants and analyzed them. NK constructed genome-editing vectors. SK, KS, and TA analyzed genome-editing efficiency. SK, YL, MT, KM, AK, HE, and TA wrote the manuscript. All authors confirmed and agreed to the content of the manuscript.

Data availability statement

The data that support the findings of this study and Materials used in this study are available from the corresponding author upon reasonable request.

Conflicts of interest

The authors declare that they have no conflicts of interest.

Supplementary data

Supplementary data is available at *Horticulture Research Journal* online.

References

1. Wiedenheft B, Sternberg SH, Doudna JA. RNA-guided genetic silencing systems in bacteria and archaea. *Nature*. 2012;**482**: 331–8.
2. Chen K, Wang Y, Zhang R. *et al.* CRISPR/Cas genome editing and precision plant breeding in agriculture. *Annu Rev Plant Biol*. 2019;**70**:667–97.
3. Ruan J, Xu J, Chen-Tsai RY. *et al.* Genome editing in livestock: are we ready for a revolution in animal breeding industry? *Transgenic Res*. 2017;**26**:715–26.
4. Jinek M, Chylinski K, Fonfara I. *et al.* A programmable dual-RNA-guided DNA endonuclease in adaptive bacterial immunity. *Science*. 2012;**337**:816–21.
5. Nishimasu H, Ran FA, Hsu PD. *et al.* Crystal structure of Cas9 in complex with guide RNA and target DNA. *Cell*. 2014;**156**: 935–49.
6. Gaudelli NM, Komor AC, Rees HA *et al.* Programmable base editing of T to G C in genomic DNA without DNA cleavage. *Nature*. 2017;**551**:464–71.
7. Nishida K, Arazoe T, Yachie N *et al.* Targeted nucleotide editing using hybrid prokaryotic and vertebrate adaptive immune systems. *Science*. 2016.
8. Muramatsu M, Kinoshita K, Fagarasan S. *et al.* Class switch recombination and hypermutation require activation-induced cytidine deaminase (AID), a potential RNA editing enzyme. *Cell*. 2000;**102**:553–63.
9. Quinlan EM, King JJ, Amemiya CT. *et al.* Biochemical regulatory features of activation-induced cytidine deaminase remain conserved from lampreys to humans. *Mol Cell Biol*. 2017;**37**.
10. Zhigang W, Smith DG, Mosbaugh DW. Overproduction and characterization of the uracil-DNA glycosylase inhibitor of bacteriophage PBS2. *Gene*. 1991;**99**:31–7.
11. Ryan MD, King AMQ, Thomas GP. Cleavage of foot-and-mouth disease virus polyprotein is mediated by residues located within a 19 amino acid sequence. *J Gen Virol*. 1991;**72**:2727–32.
12. Shimatani Z, Kashojiya S, Takayama M *et al.* Targeted base editing in rice and tomato using a CRISPR-Cas9 cytidine deaminase fusion. *Nat Biotechnol*. 2017;**35**:441–3.
13. Martinelli F, Uratsu SL, Reagan RL. *et al.* Gene regulation in parthenocarpic tomato fruit. *J Exp Bot*. 2009;**60**:3873–90.
14. Shinozaki Y, Hao S, Kojima M *et al.* Ethylene suppresses tomato (Solanum lycopersicum) fruit set through modification of gibberellin metabolism. *Plant J*. 2015;**83**:237–51.
15. Martí C, Orzáez D, Ellul P. *et al.* Silencing of DELLA induces facultative parthenocarpy in tomato fruits. *Plant J*. 2007;**52**:865–76.
16. Shinozaki Y, Beauvoit BP, Takahara M *et al.* Fruit setting rewires central metabolism via gibberellin cascades. *Proc Natl Acad Sci U S A*. 2020;**117**:23970–81.
17. Bassel GW, Mullen RT, Bewley JD. Procera is a putative DELLA mutant in tomato (Solanum lycopersicum): effects on the seed and vegetative plant. *J Exp Bot*. 2008;**59**:585–93.
18. Van De Velde K, Ruelens P, Geuten K. *et al.* Exploiting DELLA signaling in cereals. *Trends Plant Sci*. 2017;**22**:880–93.
19. Harberd NP, Belfield E, Yasumura Y. The angiosperm gibberellin-GID1-DELLA growth regulatory mechanism: how an 'inhibitor of an inhibitor' enables flexible response to fluctuating environments. *Plant Cell*. 2009;**21**:1328–39.
20. Livne S, Lor VS, Nir I. *et al.* Uncovering DELLA-independent gibberellin responses by characterizing new tomato procera mutants. *Plant Cell*. 2015;**27**:1579–94.
21. Shinozaki Y, Ezura K, Hu J. *et al.* Identification and functional study of a mild allele of SlDELLA gene conferring the potential for improved yield in tomato. *Sci Rep*. 2018;**8**:1–15.
22. Rodríguez FI, Esch JJ, Hall AE. *et al.* A copper cofactor for the ethylene receptor ETR1 from Arabidopsis. *Science*. 1999;**283**:996–8.
23. Lashbrook CC, Tieman DM, Klee HJ. Differential regulation of the tomato ETR gene family throughout plant development. *Plant J*. 1998;**15**:243–52.
24. Damayanti F, Lombardo F, Masuda J-I. *et al.* Functional disruption of the tomato putative Ortholog of HAWAIIAN SKIRT results in facultative Parthenocarpy, reduced fertility and leaf morphological defects. *Front Plant Sci*. 2019;**10**:1–18.
25. Okabe Y, Asamizu E, Saito T. *et al.* Tomato TILLING technology: development of a reverse genetics tool for the efficient isolation of mutants from micro-tom mutant libraries. *Plant Cell Physiol*. 2011;**52**:1994–2005.
26. Achard P, Genschik P. Releasing the brakes of plant growth: how GAs shutdown della proteins. *J Exp Bot* vol. **60** 1085–1092 (Oxford University Press, 2009).

27. Jiang C, Fu X. GA action: turning on de-DELLA repressing signaling. *Curr Opin Plant Biol.* 2007;**10**:461–5.

28. Li S, Zhao Y, Zhao Z. *et al.* Crystal structure of the GRAS domain of SCARECROW-LIKE7 in oryza sativa. *Plant Cell.* 2016;**28**:1025–34.

29. Hakoshima T. Structural basis of the specific interactions of GRAS family proteins. *FEBS Lett.* 2018;**592**:489–501.

30. Bleecker AB, Kende H. Ethylene: a gaseous signal molecule in plant. *Annu Rev Cell Dev Biol.* 2000;**16**:1–18.

31. Seymour GB, Chapman NH, Chew BL. *et al.* Regulation of ripening and opportunities for control in tomato and other fruits. *Plant Biotechnol J.* 2013;**11**:269–78.

32. Lacey RF, Binder BM. How plants sense ethylene gas - the ethylene receptors. *J Inorg Biochem.* 2014;**133**:58–62.

33. Kevany BM, Tieman DM, Taylor MG. *et al.* Ethylene receptor degradation controls the timing of ripening in tomato fruit. *Plant J.* 2007;**51**:458–67.

34. Wang W, Esch JJ, Shiu S-H. *et al.* Identification of important regions for ethylene binding and signaling in the transmembrane domain of the ETR1 ethylene receptor of Arabidopsis. *Plant Cell.* 2006;**18**:3429–42.

35. Ramiro AR, Barreto VM. Activation-induced cytidine deaminase and active cytidine demethylation. *Trends Biochem Sci.* 2015;**40**: 172–81.

36. Roldán-Arjona T, Ariza RR, Córdoba-Cañero D. DNA Base excision repair in plants: an unfolding story with familiar and novel characters. *Front Plant Sci.* 2019;**10**:1–18.

37. Córdoba-Cañero D, Morales-Ruiz T, Roldán-Arjona T. *et al.* Single-nucleotide and long-patch base excision repair of DNA damage in plants. *Plant J.* 2009;**60**:716–28.

38. Córdoba-Cañero D, Dubois E, Ariza RR. *et al.* Arabidopsis uracil DNA glycosylase (UNG) is required for base excision repair of uracil and increases plant sensitivity to 5-fluorouracil. *J Biol Chem.* 2010;**285**:7475–83.

39. Arazoe T, Kondo A, Nishida K. Targeted nucleotide editing Technologies for Microbial Metabolic Engineering. *Biotechnol J.* 2018;**13**:1–12.

40. Fauser F, Schiml S, Puchta H. Both CRISPR/Cas-based nucleases and nickases can be used efficiently for genome engineering in Arabidopsis thaliana. *Plant J.* 2014;**79**:348–59.

41. Sun HJ, Uchii S, Watanabe S. *et al.* A highly efficient transformation protocol for micro-tom, a model cultivar for tomato functional genomics. *Plant Cell Physiol.* 2006;**47**:426–31.